JOURNAL OF SOLID STATE CHEMISTRY 107, 149–158 (1993)

Relations between Oxygen Deficiency and Structures in the La–Sr–Cu–O System

II. A New Oxygen-Deficient Phase $(La, Sr)_4Cu_4O_{10}$

KENJI OTZSCHI AND YUTAKA UEDA

Institute for Solid State Physics, University of Tokyo, 7-22-1 Roppongi, Minato-ku, Tokyo 106, Japan

Received October 30, 1992; in revised form March 19, 1993; accepted March 22, 1993

We report the synthesis and the structural properties of a new oxygen-deficient perovskite with the formula $(La_{1-x}Sr_x)_4Cu_4O_{10}$ ($x = 0.1429$) (Sr/La = 1/6) : 4–4–10). It crystallizes in an orthorhombic cell with the parameters $a \approx 2\sqrt{2}a_p$, $b \approx \sqrt{2}a_p$, and $c \approx a_p$, where a_p means the cell constant of an ideal cubic perovskite. According to the crystal structure which has been refined in the space group *Pbam* by Rietveld analysis of powder X-ray diffraction (XRD), it has the same structure as $CaMnO_{2.5}$, and lanthanum and strontium ions in the structure are statistically distributed as well as the other compounds, $(La_{1-x}Sr_x)_8Cu_8O_{20}$ ($0.16 \leq x \leq 0.24$: 8–8–20) and $(La_{1-x}Sr_x)_5Cu_5O_{13}$ ($x = 0.1666$ (Sr/La = 1/5) : 5–5–13). This newly found 4–4–10 compound, however, is constituted by only one type of Cu–O polyhedron, i.e., CuO_5 pyramids, while the 8–8–20 and the 5–5–13 compounds include CuO_6 octahedra and/or CuO_4 squares in the structure as well. TG–DTA study and XRD measurement at high temperature revealed the structural phase transition of 4–4–10 to 8–8–20 around 550°C without any gain or loss of oxygen. Some physical properties are also reported.

1. Introduction

Oxygen-deficient perovskites which contain copper and lanthanum have been extensively studied during the last decade because of the interests in the structures and physical properties, which depend strongly on the oxygen nonstoichiometry and the ordering of oxygen vacancies. Especially since the first observation of the high T_c superconductor by Bednorz and Muller (*1*), those cuprate oxides which include CuO_2 layers in the structure have come to the fore and so much exploration for these two-dimensional compounds has been done (*2*).

During these investigations some metallic but not superconducting compounds have been found and known to have three-dimensional rather than two-dimensional structure as a result of the characteristic ordering of oxygen vacancies. For instance, $La_4Ba Cu_5O_{13}$ (4–1–5) (*3*) and $(La_{1-x}Sr_x)_8Cu_8O_{20}$ ($0.16 \leq x \leq 0.24$: 8–8–20) (*4*) have the rows of oxygen vacancies parallel to the *c*-axis and octahedral, pyramidal, and/or square planar copper coordination in the structure. The lanthanum and strontium ions in the latter compound are located in the hexagonal tunnels, which are formed by the tetragonal arrangement of the three types of copper coordination above, and distributed statistically, while in the former lanthanum and barium ions are distributed in an ordered manner over hexagonal tunnels and perovskite cages, respectively. This structural difference comes from the similarity between the ion sizes. Twelve-coordinate strontium has a close ion radius (1.58 Å) to lanthanum (1.50 Å), while barium (1.75 Å) is far larger than these cations. This can be also one of the reasons why so-called 1–2–3 superconductor exists in the

0022-4596/93 $5.00

La–Ba–Cu–O (*5, 10*) system but not in the La–Sr–Cu–O system. The 1–2–3 compounds have a cation-ordered structure.

Needless to say, these differences reflect those between the phase diagrams of these two systems. De Leeuw *et al.* investigated a more complete La_2O_3–SrO–CuO system at 950°C with reporting another new compound $La_{1+x}Sr_{2-x}Cu_2O_{5.5+\delta}$ ($0.05 \leq x \leq 0.15$) (*6*). And Wong-ng and his co-workers have studied the comprehensive phase diagrams of the R_2O_3–BaO–CuO system at 950°C, where R = lanthanides and yttrium, and reported the close correlation between phase relationships and the ionic size of R (*7*). The phases along the line with La : Sr(or Ba) = 1 : 1 for these two systems are particularly different from each other because of the existence of the compounds stated above. In addition, barium analogues for Sr_2CuO_3 (*8*) and $Sr_{14}Cu_{24}O_{41}$ (*9*) do not form, while La_2BaO_4 (*10*) is synthesized under ambient conditions, but the mutual solubility of SrO and La_2O_3 can be neglected at 950°C (*6*). In spite of these investigations the phase diagrams of the La–Sr(Ba)–Cu–O system are still preliminary. For example, another cuprate oxide $(La_{0.25}Sr_{0.75})_8Cu_8O_{18-\delta}$ (δ = 0.4, 2.0 : 8–8–18) (*11–13*) has been recently synthesized by Fu *et al.*, which has turned out to be an oxygen-deficient perovskite. Moreover, investigations on phase equilibria under various conditions, i.e., temperature, pressure, and so on, have scarcely been carried out.

Recently, we have reported a new oxygen deficient perovskite $(La_{1-x}Sr_x)_5Cu_5O_{13}$ (x = 0.1666 (Sr/La = 1/5) : 5–5–13) (*14*), which is synthesized by hot isostatic pressing (HIP; P_{O_2} = 300 atm, 600°C, 6 hr) of $(La_{1-x}Sr_x)_8Cu_8O_{20}$ and has an analogous structure to 4–1–5, where the statistical distribution of lanthanum and strontium occurs. We also reported the wide solid solution range of x in 8–8–20 compound. Along these studies we isolated a new compound which crystallizes in an orthorhombic cell with the parameters $a \approx 2\sqrt{2}a_p$, $b \approx \sqrt{2}a_p$, and $c \approx a_p$, where a_p means the cell constant of an ideal cubic perovskite. This newly found compound has the formula $(La_{1-x}Sr_x)_4Cu_4O_{10}$ (x = 0.1429 (Sr/La = 1/6) : 4–4–10) and exhibits the phase transition to the 8–8–20 phase around 550°C. The Rietveld refinement on its powder X-ray diffraction pattern revealed that it is isostructural to the manganese perovskites, $CaMnO_{2.5}$ (*15–17*) and $Sr_2Mn_2O_5$ (*18, 19*). In this paper we report the preparation, the refined structure and the phase transition of this compound. The solid solution range of x and some physical properties are also reported.

2. Experimental

All samples were prepared by solid-state reaction in an alumina crucible covered with platinum foil from appropriate mixtures of predried La_2O_3, $SrCO_3$, and CuO in a ratio of $(1 - x)/2 : x : 1$ (x = 0.0, 0.05, 0.10, 0.125 (=1/8), 0.1429 (=1/7), 0.15, 0.1666 (=1/6), 0.2 (=1/5), 0.2381 (=1/3.2), and 0.25 (=1/4)). The mixtures were first decarbonated in air at 900°C for several hours. Then the powders were reground, pressed into pellets, sintered under flowing oxygen gas at 1025°C for 16 hr and cooled to room temperature slowly in the furnace. These treatment were repeated two more times.

Powder X-ray diffraction patterns were collected using a Mac Science MXP^{18} system with a rotating anode generator and a monochromator of single crystalline graphite for Cu-$K\alpha$ radiation. A Mac Science High Temperature XRD Equipment was used to observe the phase transition *in situ*. The Rietveld refinement was made by the analysis program RIETAN (*20*) in the range 2θ = 20–116° with a step of 0.02°.

The oxygen contents and nonstoichiometry were obtained by thermogravimetric and differential thermal analysis using a Mac Science TG-DTA 2000 assembly under flowing diluted hydrogen gas (5% H_2/N_2) or oxygen gas (99.9995%). The weight loss by hydrogen reduction gives the composition of oxygen assuming that the compound is

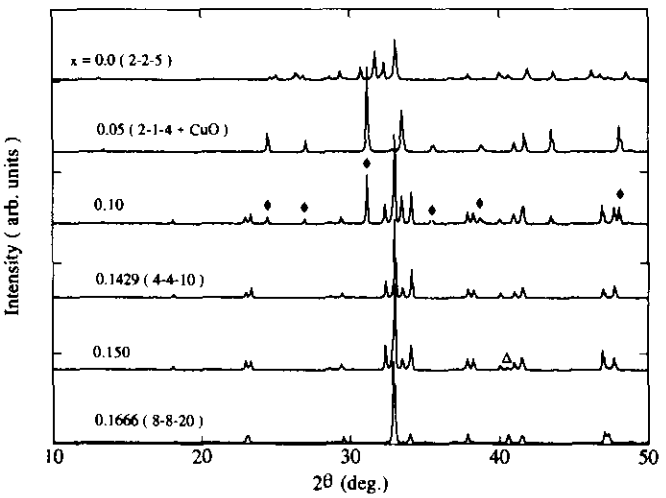

FIG. 1. X-ray powder diffraction patterns for the samples with the compositions $\frac{1}{2}La_2O_3 : SrO : CuO = 1 - x : x : 1$, $x = 0.0$, 0.05, 0.10, 0.1429 (=$\frac{1}{7}$), 0.15, and 0.1666 (=$\frac{1}{6}$) reacted at 1025°C under 1 atm of oxygen and cooled slowly to room temperature. The $x = 0.0$, 0.1429, and 0.1666 samples are the single-phase compounds, $La_2Cu_2O_5$ (2–2–5), $(La_{0.8571}Sr_{0.1429})_4Cu_4O_{10}$ (4–4–10, see text), and $(La_{0.8333}Sr_{0.1666})_8Cu_8O_{20}$ (8–8–20), respectively. The $x = 0.05$ sample is a mixture of $(La, Sr)_2CuO_4$ (2–1–4) and CuO. The $x = 0.10$ sample consists of the 2–1–4 (◆), CuO, and the 4–4–10 compounds. The $x = 0.150$ sample contains mainly the 4–4–10 compound with a small quantity of the 8–8–20 (Δ).

finally decomposed into a mixture of Cu-metal, SrO, and La_2O_3.

The electrical resistivity measurements were carried out by the four probe method in the range 5–280 K at 1 K intervals. The magnetic susceptibility was measured by the conventional Faraday method in $H_{ext} = 11.8$ kOe in the temperature range 4.2–300 K.

3. Results and Discussion

Phase Relations

X-ray powder diffraction (XRD) patterns for the samples, which were cooled slowly in the furance down to room temperature, with varying strontium concentration x in the perovskite formula $La_{1-x}Sr_xCuO_y$ are shown in Fig. 1, and the phases contained in these compositions are listed in Table I. A first attention is given to the pretty difference between the XRD patterns for the $x = 0$ sample and the others. The $x = 0$ sample shows no reflections which are due to perovskite lattice. De Leeuw *et al.* reported that this composition is in a two-phase region (La_2CuO_4 + CuO) at 950°C in 1 bar of oxygen (*6*), but Cava *et al.* (*21*) made it clear that the single-phase $La_2Cu_2O_5$ (2–2–5) ex-

TABLE I

PHASES IN $(La_{1-x}Sr_x)CuO_y$'' PREPARED AT 1025°C IN O_2

x	Phases
0.00	2–2–5[a]
0.05	2–1–4[b] + CuO
0.10	2–2–4[b] + CuO + New phase
0.125	New phase + 2–1–4[b] + CuO
0.1429	New phase
0.15	New phase + 8–8–20[c]
0.1666	8–8–20[c]
0.20	8–8–20[c]
0.2381	8–8–20[c]
0.25	8–8–20[c]

Note. Each code represents [a] $La_2Cu_2O_5$, [b] $(La, Sr)_2CuO_4$, and [c] $(La_{1-x}Sr_x)_8Cu_8O_{20}$, respectively.

ists at higher temperature (999–1012°C) in air. Despite the extremely restricted conditions as they described, our preparation method (at 1025°C in oxygen and furnace-cooled) also gave this 2–2–5 compound. It is interesting that 2–2–5 shows a quite different XRD pattern from perovskite but has a La_2CuO_4-like unit in the structure. The compound 2–2–5, however, may exist only in a very narrow strontium substitution range as well as the extremely restricted temperature region. Replacement of only 5% of lanthanum by strontium leads the system to two-phase region (2–1–4 + CuO). The structure of 2–2–5 would be very sensitive to the ion radius of the cation, which is the weighted average of the ion radii of lanthanum and strontium in the present case supposing that these cations are distributed statistically on the analogy of other cuprates (ex. 8–8–20, 5–5–13), and a slight increase of it can be fatal for the structure.

More substitution of strontium for lanthanum results in the formation of the titled compound, which is new oxygen-deficient perovskite in the La–Sr–Cu–O system as described below. The single-phase region of this newly found compound is tremendously narrow and only $x = 0.1429$ composition (Sr/La = 1/6) in our samples gives the single phase. The samples with $x = 0.125$ and 0.15 contain 2–1–4 and 8–8–20 phase, respectively, as an impurity. The reflections for this compound can be indexed in an orthorhombic system with the cell constants $a = 10.5028(5)$ Å $\approx 2\sqrt{2}a_p$, $b = 5.5264(3)$ Å $\approx \sqrt{2}a_p$ and $c = 3.8654(2)$ Å $\approx a_p$ at room temperature. In electron diffraction (ED) observation, some crystals showed extra spots corresponding to the superstructure, $b \approx 2\sqrt{2}a_p$ or $c \approx 2a_p$, but no extra lines attributed to these superstructures were observed on the XRD pattern (*4*). Table II shows the indexing for the reflections and relative intensity of diffraction.

Er-Rakho *et al.* (*4*) have reported a wide solid solution range ($0.16 \leq x \leq 0.24$) for the 8–8–20 phase. On the other hand, our sample with $x = 0.15$ contains mainly the new phase. This means the relatively narrow two-phase region between 8–8–20 and the new phase.

TABLE II

INDICES AND INTENSITY OF POWDER XRD PATTERN (Cu-$K_{\alpha 1}$) FOR $(La_{0.8571}Sr_{0.1429})_4Cu_4O_{10}$ IN AN ORTHORHOMBIC UNIT CELL

h	k	l	I/I_0	$2\theta_{obs}$	$2\theta_{calc}$
0	0	1	7	22.94	22.93
2	1	0	9	23.32	23.29
2	0	1	2	28.62	28.59
1	1	1	7	29.38	29.36
3	1	0	1	30.14	30.13
0	2	0	22	32.32	32.31
2	1	1	100	32.96	32.94
1	2	0	11	33.46	33.45
4	0	0	24	34.08	34.06
4	1	0	11	37.86	37.85
3	1	1	11	38.24	38.23
0	2	1	6	40.04	40.02
1	2	1	11	40.98	40.97
4	0	1	10	41.52	41.48
2	2	1	1	43.70	43.71
4	1	1	1	44.74	44.74
0	0	2	20	46.92	46.92
4	2	0	18	47.70	47.68
1	3	0	1	50.20	50.18
1	1	2	1	50.70	50.69
5	1	1	1	52.16	52.15
2	1	2	3	53.06	53.04
4	2	1	1	53.58	53.57
5	2	0	4	54.80	54.80
1	3	1	9	55.88	55.88
3	3	0	4	56.34	56.33
6	0	1	4	57.72	57.71
0	2	2	9	58.14	58.15
1	2	2	5	58.86	58.87
4	0	2	11	59.28	59.26

Oxygen Contents

The oxygen contents of 8–8–20 compounds ($x = 0.1666$, 0.2, 0.2381, and 0.25) and the new compounds ($x = 0.1429$ and 0.125) are determined by thermogravimetric analysis (TGA) and the results are summarized in Table III. It is noted that the 8–8–20 phase has the same oxygen content 20.0 independent of x, that is, the general formula $(La_{1-x}Sr_x)_8Cu_8O_{20-\varepsilon}$ ($\varepsilon = 0.0$). Er-Rakho *et*

TABLE III
OXYGEN CONTENTS DETERMINED BY TGA

Formula	x	ε
$(La_{1-x}Sr_x)_8Cu_8O_{20-\varepsilon}$	0.1666	0.00 ± 0.02
	0.200	0.02 ± 0.02
	0.2381	0.00 ± 0.03
	0.250	−0.02 ± 0.02
$(La_{1-x}Sr_x)_4Cu_4O_{10-\varepsilon}$	0.1429	0.00 ± 0.03
	0.125	−0.02 ± 0.02

al. reported increase of oxygen deficiency with increasing strontium concentration x (*4*). This difference can be due to the synthesis conditions or the method of ε determination. They prepared the samples in air and adopted the redox back titration (Fe(II)/Fe(III)) for analysis. In our latest paper (*14*), we reported the oxygen nondeficiency of $(La_{0.8333}Sr_{0.1666})_8Cu_8O_{20}$ up to considerably high temperature (~1080°C) in air or flowing oxygen gas. This stoichiometry also holds against substitution of strontium according to our results.

The newly found compound turned out to have the formula $((La_{1-x}Sr_x)_4Cu_4O_{10-\varepsilon}$ (4–4–10) by TGA. This 4–4–10 compound can be considered to be also stoichiometric ($\varepsilon \sim 0.0$), though only two compositions ($x = 0.1429$ and 0.125) have been tried. In addition, the TG curve for it in air or flowing oxygen gas is almost the same for 8–8–20. Weight loss begins around 1030°C on heating with rate 5°C/min. The resultant powder contained 2–1–4 compound and CuO as well as the case of 8–8–20 (*14*).

Rietveld Refinement of the 4–4–10 Structure

We obtained the cell parameters ($2\sqrt{2}a_p \times \sqrt{2}a_p \times a_p$) and the composition (4–4–10) of the new compound from XRD and TGA, then we tried the structure refinement using Rietveld analysis. Two space groups, *Pbam* and *Pba*2, are possible because of the conditions on observable reflections $h0l: h = 2n$, $0hl: k = 2n$, ($h00: h = 2n$), ($0k0: k = 2n$). At the beginning, in order to minimize the number of variable parameters more symmetric space group *Pbam* was chosen. The calculations were started with a composition without any vacancies, that is, an ideal perovskite $(La_{0.8571}Sr_{0.1429})_4Cu_4O_{12}$. The starting positions for different atoms were given from this ideal structure (see Table IV). Lanthanum and strontium were distributed statistically because there is only one site for these cations. First, all the isotropic thermal parameters were fixed to 1.0 Å^2. After refinements of background, peak-profile and cell parameters and scale factor with fixed atomic parameters, R_i (integrated intensity R-factor) was reduced to 0.2677, which implies the justice in perovskite structure model. Then the positions of La(Sr) and Cu were refined, but following refinement of positions of oxygen atoms failed. In this step, the oxygen vacancies were considered. With regard to the formula (La, Sr)$_4$Cu$_4$O$_{10}$, two oxygen atoms had to be removed from the unit cell. This number corresponds to that of O(1) or O(2) oxygen, then the occupancy factors on these sites were refined. For simplicity, partial removal of oxygen from other sites was neglected. The occupancies on O(1) and O(2) sites converted to 1.0 and 0.0 respectively and therefore O(2) was omitted. After the final refinement with each isotropic thermal parameters for each kind of atoms the discrepancy factor converged to $R_i = 0.0356$ ($R_p = 0.0535$, $R_e = 0.0339$, and $R_{wp} = 0.0743$), and atomic parameters are given in Table IV. Figure 2 shows the observed and calculated XRD profiles. Further refinement using the lower symmetric space group *Pba*2 slightly reduced the R-factor but the changes of related atomic parameters, i.e., z coordination, were in accord with *Pbam* within the standard deviations.

By the structural refinement described above, the 4–4–10 phase is revealed to have the same structure as Ca(or Sr)MnO$_{2.5}$ (*15–19*), which is synthesized by the reduction of the perovskites Ca(or Sr)MnO$_3$ with

TABLE IV

STARTING AND FINALLY REFINED ATOMIC PARAMETERS FOR $(La_{0.8571}Sr_{0.1429})_4Cu_4O_{16}$ IN THE SPACE GROUP *Pbam*[c,d]

Atom	Sites	x^a	y^a	z^a	x^b	y^b	z^b	B (Å^2)[b,e]
La(Sr)	4*h*	0.125	0.75	0.5	0.1397(5)	0.8111(8)	0.5	1.40(11)
Cu	4*g*	0.125	0.25	0	0.105(1)	0.287(2)	0	2.20(21)
O(1)	2*a*	0	0	0	0	0	0	1.80(48)
O(2)	2*c*	0	0.5	0		0.072(6)		
O(3)	4*g*	0.25	0	0	0.283(3)	0.288(7)	0	
O(4)	4*h*	0.125	0.25	0.5	0.093(3)		0.5	

[a] Starting positions.
[b] Refined parameters.
[c] Lattice constants: a = 10.5028(5) Å, b = 5.5264(3) Å, c = 3.8654(2) Å.
[d] Discrepancy factors: R_i = 0.0356, R_p = 0.0535, R_{wp} = 0.0743, R_e = 0.0339.
[e] The common thermal parameter is used for oxygen atoms.

hydrogen gas or zirconium metal. Selected distances between metal (La(Sr) and Cu) and oxygen atoms are listed in Table V and a schematic projection of the polyhedral framework of it onto the (100) plane is shown in Fig. 3. A characteristic is that only one kind of copper (or manganese), which is pyramidally five-coordinated, exists in this structure, while two or three types of copper coordination are contained in the 5–5–13 or 8–8–20 structure (*4*, *14*). Another oxygen-deficient perovskite 8–8–18 has recently been reported to have also one kind of coordination, i.e., pyramidal, by Fujishita *et al.* (*13*) but Fu *et al.*'s solution was in disagreement with their results (*12*). All distances listed in Table V are suitable for usually observed cuprate oxides. CuO_5 pyramids

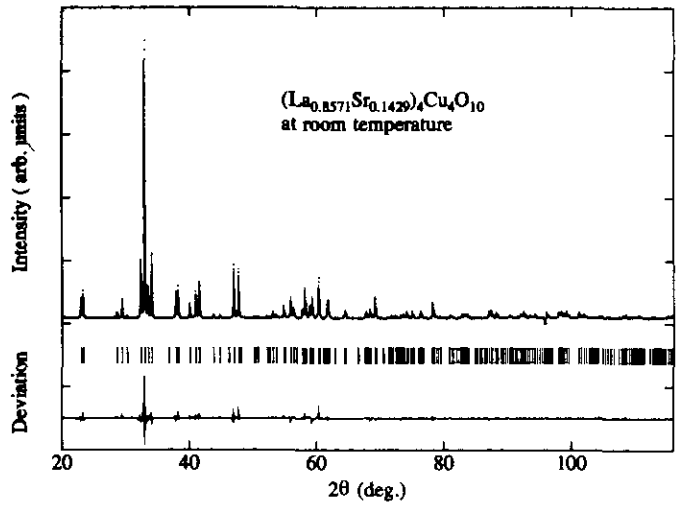

FIG. 2. X-ray Rietveld refinement pattern for $(La_{0.8571}Sr_{0.1429})_4Cu_4O_{10}$ at room temperature. The observed and the calculated data is shown by a continuous line and by dots, respectively. The difference between them is shown in the lower portion. The bars drawn in the middle portion show the positions of the reflection peaks attributed to the space group *Pbam*.

TABLE V

INTERATOMIC DISTANCES IN $(La_{0.8571}Sr_{0.1429})_4Cu_4O_{10}$

M–O		Distance (Å)
Cu–O(1)[a]	×1	1.930(2)
Cu–O(3)[a]	×1	2.213(5)
Cu–O(3)[b]	×1	1.969(5)
Cu–O(4)[a]	×2	1.936(1)
La(Sr)–O(1)[c]	×2	2.641(1)
La(Sr)–O(3)[b]	×2	2.478(3)
La(Sr)–O(3)[c]	×2	2.83(4)
La(Sr)–O(4)[a]	×1	2.932(5)
La(Sr)–O(4)[b]	×1	2.810(5)
La(Sr)–O(4)[d]	×1	2.505(5)
La(Sr)–O(4)[b]	×1	2.680(5)

Note. Symmetry codes: [a] x, y, z; [b] $\frac{1}{2} - x, \frac{1}{2} + y, z$; [c] $x, 1 + y, z$; [d] $-x, 1 - y, z$.

have one longer Cu–O distance (2.21 Å), which is on the side opposite to the oxygen vacancy, than the other four (1.93–1.97 Å). This distortion is also observed for $CaMnO_{2.5}$ (*15, 16*) and $La_4BaCu_5O_{12}$ (*3*), but not for $Sr_2Mn_2O_5$ (*18*), and results from unequal electron occupancy of the d_{z^2} and $d_{z^2-y^2}$ orbitals (*3, 15*). These pyramids rotate around the oxygen vacancy and therefore the arrangement of 10 oxygen atoms around La(Sr) species is pretty distorted. Two La(Sr) atoms in the same hexagonal tunnel move away from each other as well in the 5–5–13 structure.

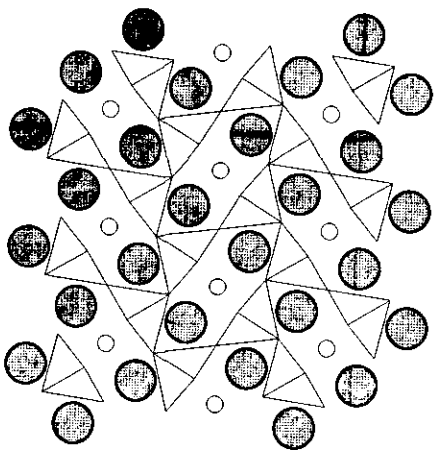

FIG. 3. A schematic projection onto the (001) plane of the framework of $(La_{0.8571}Sr_{0.1429})_4Cu_4O_{10}$. Large shaded circles stand for La(Sr) and triangles show the arrangement of CuO_5 pyramids. Oxygen vacancies are represented by small open circles. CuO_5 pyramids are distorted around the oxygen vacancies, and two La(Sr) atoms located in the same hexagonal tunnel move in directions opposite to each other away from the oxygen vacancy.

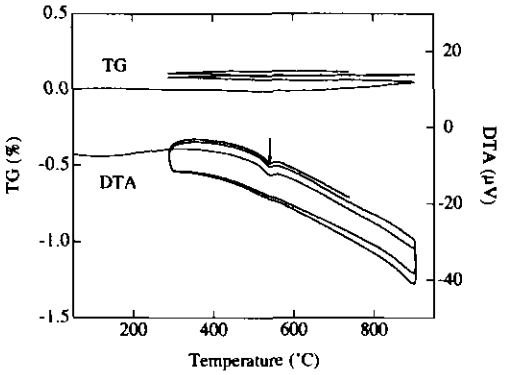

FIG. 4. TG and DTA curves for the $x = 0.1429$ sample heated/cooled at 5°C/min in flowing oxygen gas. An endothermic peak was observed on heating (arrow), but a corresponding exothermic peak on cooling was not clear.

Phase Transition from the 4–4–10 to the 8–8–20

In the TG–DTA measurement for the $x = 0.1429$ sample in air or flowing oxygen gas, an endothermic peak was also observed in the differential thermal analysis (DTA) curve around 550°C. This peak appears only on heating but not on cooling, and was reobservable along several repeats of heating and cooling (see Fig. 4). We considered that this anomaly was due to a certain structural phase transition, and then X-ray powder diffraction measurement at high temperature (HT–XRD) was carried out. The results are that the 4–4–10 compound with $x = 0.1429$ changes into the 8–8–20 phase with little gain or loss of oxygen. This is the first observation of the phase transition from one oxygen-deficient phase to the other without a gain or loss of oxygen in La–Sr(Ba)–Cu–O

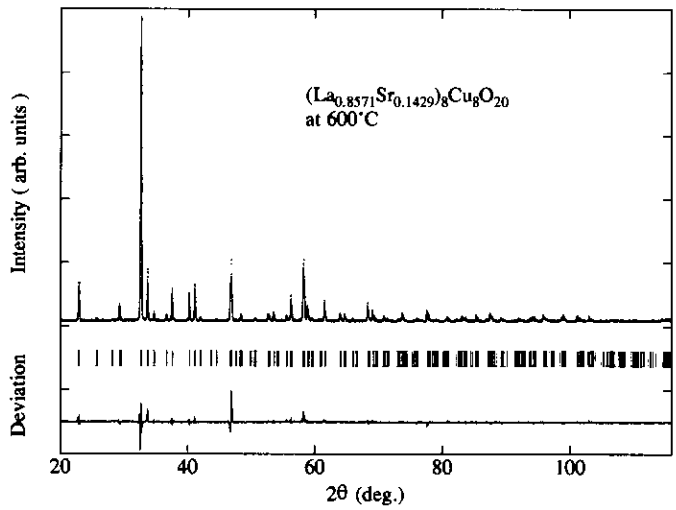

FIG. 5. X-ray Rietveld refinement pattern for $(La_{0.8571}Sr_{0.1429})_8Cu_8O_{20}$ at 600°C. The observed and the calculated data is shown by a continuous line and by dots, respectively. The difference between them is shown in the lower portion. The bars drawn in the middle portion show the positions of the reflection peaks attributed to the space group *P4/mbm*.

system. The two-phase (4–4–10 + 8–8–20) region lies in the temperature range from 500 to 580°C on heating and from 560 to 320°C on cooling. The bare peak in DTA curve on cooling comes from this far wider two-phase area on cooling than that on heating.

The structure of this high-temperature phase $(La_{1-x}Sr_x)_8Cu_8O_{20}$ (x = 0.1429) was refined for powder XRD at 600°C by Rietveld analysis in the same way as in Ref. (*4*), where the space group *P4/mbm* was chosen to minimize the number of variable parameters (see Fig. 5). The refined cell constants are a = 10.9581(5) Å $\approx 2\sqrt{2}a_p$ and c = 3.8879(2) Å $\approx a_p$ and the discrepancy factor was finally reduced to R_i = 0.0529 (R_p = 0.0630, R_e = 0.0507, and R_{wp} = 0.0868). The finally refined atomic parameters and interatomic distances are listed in Tables VI and VII, respectively. The atomic parameters are almost the same as Er-Rakho's first report for the 8–8–20 phase and the values of interatomic distances are compatible with those usually observed in the cuprate oxides.

Electrical and Magnetic Properties

Figure 6 shows the temperature dependence of the electrical resistivity of the samples with x = 0.1429 and 0.125. The new compound 4–4–10 exhibits metallic behavior and measurements down to 5 K shows no evidence of superconductivity. An anomaly around 30–40 K is due to the superconducting impurities (2–1–4 phase). Another broad anomaly was noted for the x = 0.1429 sample around the upper limit of the observation

TABLE VI

ATOMIC PARAMETERS FOR $(La_{0.8571}Sr_{0.1429})_8Cu_8O_{20}$ AT 600°C IN THE SPACE GROUP *P4/mbm*[a,b]

Atom	Sites	x	y	z	B (Å^2)[c]
La(Sr)	8*j*	0.2617(4)	0.4681(4)	0.5	1.37(12)
Cu(1)	2*a*	0	0	0	1.22(22)
Cu(2)	2*d*	0.5	0	0	
Cu(3)	4*g*	0.2197(10)	0.5 + x	0	
O(1)	2*b*	0	0	0.5	2.24(66)
O(2)	2*c*	0.5	0	0.5	
O(3)	4*h*	0.198(4)	0.5 × x	0.5	
O(4)	4*g*	0.380(4)	0.5 + x	0	
O(5)	8*i*	0.163(4)	0.082(4)	0	

[a] Lattice constants: a = 10.9581(5) Å, c = 3.8879(2) Å.

[b] Discrepancy factors: R_i = 0.0529, R_p = 0.0630, R_{wp} = 0.0868, R_e = 0.0507.

[c] The common thermal parameter is used for copper and oxygen atoms each.

TABLE VII

INTERATOMIC DISTANCES IN $(La_{0.8571}Sr_{0.1429})_8Cu_8O_{20}$ AT 600°C

Cu(1)–O(1)[a]	×2	1.944(1)
Cu(1)–O(5)[a]	×4	2.003(10)
Cu(2)–O(2)[a]	×2	1.944(1)
Cu(2)–O(4)[d,e]	×2	1.865(14)
Cu(3)–O(3)[a]	×2	1.974(3)
Cu(3)–O(4)[a]	×1	2.479(14)
Cu(3)–O(5)[b,f]	×2	1.979(10)
La(Sr)–O(1)[b]	×1	2.635(2)
La(Sr)–O(2)[b]	×1	2.889(2)
La(Sr)–O(3)[a]	×1	2.611(7)
La(Sr)–O(3)[c]	×1	2.997(11)
La(Sr)–O(4)[c]	×2	2.667(2)
La(Sr)–O(5)[b]	×2	2.453(6)
La(Sr)–O(5)[g]	×2	2.963(8)

Note. Symmetry codes: [a] x, y, z; [b] $\frac{1}{2} - x, \frac{1}{2} + y, z$; [c] $\frac{1}{2} - x, -\frac{1}{2} + y, z$; [d] $1 - x, 1 - y, z$; [e] $x, y - 1, z$; [f] $y, 1 - x, z$; [g] $\frac{1}{2} - y, \frac{1}{2} - x, z$.

temperature. It is noted that the 4–4–10 shows metallic resistivity, while the isotypical $Sr_2Mn_2O_5$ is an insulator because of the antiferromagnetical ordering of Mn(III) spins below room temperature (*18*). The resistivity of the 4–4–10 phase tends to increase with increasing strontium concentration, which is an opposite behavior from the 8–8–20 phase (*14*). The large resistivity in comparison with other metallic cuprates comes from poor sinterability of this compound.

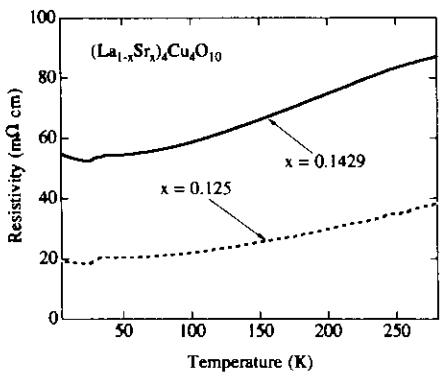

FIG. 6. Temperature dependence of electrical resistivity for the samples with $x = 0.1429$ and 0.125. An anomaly around 30–40 K is caused by small quantities of the superconducting second phase. Measurements down to 5 K show no evidence of superconductivity for either composition.

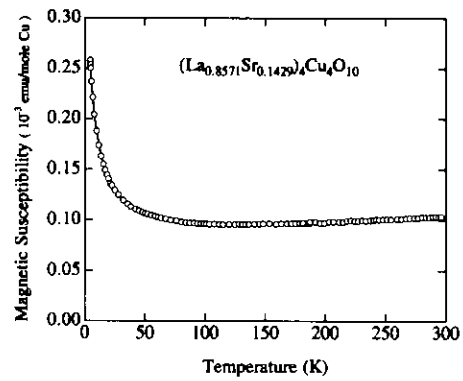

FIG. 7. Magnetic susceptibility of $(La_{0.8571}Sr_{0.1429})_4Cu_4O_{10}$ as a function of temperature.

The temperature dependence of the magnetic susceptibility of the $x = 0.1429$ sample is shown in Fig. 7. The weak temperature dependence along higher temperature implies a Pauli paramagnetic nature of it, which is in the same order of magnitude as those of other metallic cuprates, but a slight increase of the susceptibility with increasing temperature above 100 K is noticeable because such behavior has not observed for other compounds, for example, the 5–5–13 and the 8–8–18 phase (*13, 14*). It is not obvious at present whether the increase as decreasing temperature below 50 K is due to the existence of magnetic impurities or is an intrinsic property.

The microscopic study on the electronic state of the compound by NMR and NQR is now in progress.

4. Conclusion

The newly isolated compound is formulated to be $(La_{1-x}Sr_x)_4Cu_4O_{10-\varepsilon}$ (4–4–10) by TG analysis, where oxygen nonstoichiometry ε is almost zero. This phase exists only in the narrow range of strontium concentra-

tion x around 0.1429 (=1/7) and the samples with $x = 0.125$ and 0.15 contain the second-phase impurities, which are $(La, Sr)_2CuO_{4+\varepsilon}$ (2–1–4)/CuO and $(La_{1-x}Sr_x)_8Cu_8O_{20-\varepsilon}$ (8–8–20), respectively. The structure is of an oxygen-deficient perovskite whose oxygen vacancy ordering is the same as $CaMnO_{2.5}$ and includes only one sort of CuO_n polyhedra, i.e., CuO_5 pyramids, while the 8–8–20 and the 5–5–13 compounds contain CuO_6 octahedra and/or CuO_4 squares. Lanthanum and strontium ions in the structure are statistically distributed over hexagonal tunnels. This compound shows metallic conductivity and Pauli paramagnetism as well as other three-dimensional cuprate oxides and measurements down to 5 K show no evidence of superconductivity. The compound shows the stuctural phase transition to the 8–8–20 phase around 550°C without any oxygen loss or gain.

The oxygen deficiencies ε of the 4–4–10 and the 8–8–20 phases are almost stoichiometric ($\varepsilon = 0$) independent of both temperature and x.

Now we are researching the phase diagram on the "perovskite line" $SrCuO_2$–$La_2Cu_2O_5$ in the lanthanum-rich region and the composition dependence of the phase transition temperature from the 4–4–10 to the 8–8–20.

Acknowledgments

The authors are grateful to Dr. A. Hayashi for assistance and to Mr. K. Koga for measurement of magnetic susceptibility. They also thank Dr. K. Suzuki for electron microscopy observations. This work was partly supported by a Grant-in-Aid for Scientific Research on Priority Areas, "Science of High T_c Superconductivity," given by the Ministry of Education, Science, and Culture of Japan.

References

1. J. G. Bednorz and K. A. Muller, *Z. Phys. B* **64,** 189 (1986).
2. J. B. Torrance, Y. Tokura, A. Nazzal, and S. S. P. Parkin, *Phys. Rev. Lett.* **60,** 542 (1988) and literatures therein.
3. C. Michel, L. Er-Rakho, M. Hervieu, J. Pannetier, and B. Raveau, *J. Solid State Chem.* **68,** 143 (1987).
4. L. Er-Rakho, C. Michel, and B. Raveau, *J. Solid State Chem.* **73,** 514 (1988).
5. (a) W. I. F. David, W. T. A. Harrison, R. M. Ibberson, M. T. Weller, J. R. Grasmeder, and P. Lanchester, *Nature* **328,** 328 (1987); (b) C. V. Segre, B. Dabrowski, D. G. Hinks, K. Zhang, J. D. Jorgensen, M. A. Beno, and Ivan K. Schuller, *Nature* **329,** 227 (1987).
6. D. M. De Leeuw, C. A. H. A. Mutsaers, G. P. J. Geelen, and C. Langereis, *J. Solid State Chem.* **80,** 276 (1989).
7. W. Wong-ng, B. Paretzkin, and E. R. Fuller, Jr., *J. Solid State Chem.* **85,** 117 (1988).
8. H. Müller-Buschbaum, *Angew. Chem.* **89,** 704 (1977).
9. E. M. McCarron, M. A. Subramarian, J. C. Calabrese, and R. L. Harlow, *Mater. Res. Bull.* **23,** 1355 (1988).
10. D. Klibanow, K. Sujata, and T. O. Mason, *J. Am. Ceram. Soc.* **71,** C267 (1988).
11. W. T. Fu, Q. Xu, A. A. Verheijen, J. M. von Ruitenbeek, H. W. Zandbergen, and L. J. de Jongth, *Solid State Commun.* **73,** 291 (1990).
12. W. T. Fu, F. C. Mijlhoff, D. J. W. Ijdo, and V. Ponec, *Solid State Commun.* **83,** 59 (1992).
13. H. Fujishita, M. Sera, and M. Sato, *Physica C* **175,** 165 (1991).
14. K. Otzschi, A. Hayashi, Y. Fujiwara, and Y. Ueda, *J. Solid State Chem.*, in press.
15. K. R. Poeppelmeier, M. E. Leonowicz, and J. M. Longo, *J. Solid State Chem.* **44,** 89 (1982).
16. K. R. Poeppelmeier, M. E. Leonowicz, J. C. Scanlon, J. M. Longo, and W. B. Yelon, *J. Solid State Chem.* **45,** 71 (1982).
17. A. Reller, J. M. Thomas, F. R. S, D. A. Jefferson, and M. K. Uppal, *Proc. R. Soc. London Ser. A* **394,** 223 (1984).
18. V. Caignaert, N. Nguyen, M. Hervieu, and B. Raveau, *Mater. Res. Bull.* **20,** 479 (1985).
19. V. Caignaert, M. Hervieu, N. Nguyen, and B. Raveau, *J. Solid State Chem.* **62,** 281 (1986).
20. F. Izumi, *J. Crystallogr. Soc. Jpn.* **27,** 23 (1985).
21. R. J. Cava, T. Siegrist, B. Hessen, J. J. Krajewski, W. F. Peck, Jr., B. Batlogg, H. Takagi, J. V. Waszczak, L. F. Schneemeyer, and H. W. Zandbergen, *J. Solid State Chem.* **94,** 170 (1991).